CHEST

Thoracic involvement in Erdheim-Chester disease: computed tomography imaging findings and their association with the *BRAF*^V600E mutation

S. Mojdeh Mirmomen[1] · Arlene Sirajuddin[2] · Moozhan Nikpanah[1] · Rolf Symons[1] · Anna K. Paschall[1] ·
Ioannis Papageorgiou[4] · William A. Gahl[3] · Kevin O'Brien[3] · Juvianee I. Estrada-Veras[3] · Ashkan A. Malayeri[1]

Abstract

Objectives To investigate the computed tomography (CT) thoracic findings in Erdheim-Chester disease (ECD) and evaluate the association of these findings with the *BRAF*^V600E mutation.

Methods This was a prospective study of patients with ECD (n=61, men=46) who underwent thoracic CT imaging. CT examinations were independently interpreted by two experienced radiologists. Association of imaging findings with *BRAF*^V600E was achieved via the Chi-square or Fisher's exact test and odds ratios (OR) with 95% confidence intervals (CI), as appropriate.

Results Fifty-five ECD patients (90%) showed pulmonary findings, which included interlobular septal thickening (69%), pulmonary nodules (62%), airway thickening (13%) and ground glass opacities (36%). Pulmonary nodules were classified by the pattern of distribution: subpleural regions (36%), lung parenchyma (13%) and both regions (13%). Pleural and mediastinal involvement were present in 15% and 62% of cases, respectively. The most common mediastinal finding was sheathing of the right coronary artery (34%), followed by sheathing of the thoracic aorta (30%). The *BRAF*^V600E mutation, positive in 31 patients, was associated with the frequency of sheathing of the coronary arteries ($p = 0.01$).

Conclusions Of the thoracic findings reported in this study, we found a statistically significant positive association between the *BRAF*^V600E mutation and presence of coronary artery sheathing.

Key Points

• *To assess the degree of thoracic involvement in ECD with CT.*
• *BRAF*^V600E *mutation has a high association with right coronary artery sheathing.*
• *BRAF*^V600E *genetic testing detects patients at high risk of developing RCA sheathing.*

✉ Ashkan A. Malayeri
  ashkan.malayeri@nih.gov

1 Radiology and Imaging Sciences, National Institutes of Health Clinical Center, 10 Center Dr, Bethesda, MD 20892, USA

2 National Heart, Lung, and Blood Institute, National Institutes of Health, Bethesda, MD, USA

3 National Human Genome Research Institute, Medical Genetics Branch, Office of the Clinical Director, National Institutes of Health Clinical Center, Bethesda, MD, USA

4 Magnetic Resonance Imaging of Epirus (Magnitiki Tomografia Ipirou), Ioannina, Greece

Abbreviations

CI	Confidence interval
CT	Computed tomography
ECD	Erdheim-Chester disease
ERK	Extracellular signal-regulated kinase
HIPPA	Health Insurance Portability and Accountability Act
LCH	Langerhans cell histiocytosis
MAP	Mitogen-activated protein
MDCT	Multi-detector computed tomography
NHGRI	National Human Genome Research Institute
OR	Odds ratio
RCA	Right coronary artery
SD	Standard deviation
WHO	World Health Organization

Introduction

Erdheim-Chester disease (ECD) is a rare, sporadic, non-Langerhans cell histiocytosis [1, 2]. First described in 1930 by William Chester and Jakob Erdheim, ECD was reclassified as a histiocytic neoplasm by the World Health Organization (WHO) in 2016. This multisystemic disorder presents with a range of clinical symptoms and the prognosis varies, depending on the extent and distribution of the lesions. Since the discovery of ECD, over 500 patients have been reported worldwide, with more than 300 new cases diagnosed in the past 10 years [1–5]. Although the ages of the ECD patients ranged from 7 to 84 years, patients are most commonly diagnosed between the fifth and seventh decades of life, and have a male predominance [4, 6].

The skeletal system is the most frequently involved in ECD; however, extra-skeletal involvement in the chest, abdomen and pelvis has been reported in more than 50% of patients [1, 7]. Various clinical and radiological manifestations can suggest ECD, but definitive diagnosis requires biopsy and tissue analysis. ECD is characterized by the deposition of foamy (lipid-laden macrophages) or epithelioid histiocytes within the affected tissues surrounded by variable areas of fibrosis on histopathology [6, 7]. The histiocytes of ECD stain positive for CD68 and CD163, and negative for CD1a; most ECD cases also stain negative for S100. This immune profile differentiates ECD from Langerhans cell histiocytosis (LCH), a more common histiocytic disorder that stains positive for CD68, CD1a and S100 [1, 3, 6–8]. Moreover, half of ECD patients have the $BRAF^{V600E}$ mutation, a proto-oncogene that activates mitogen-activated protein (MAP) kinase and extra-cellular signal-regulated kinase (ERK) signalling pathways. Pathogenic variations in these regulatory pathways lead to the development of many cancers [9–11]. Recently, $BRAF$ inhibitor therapy has shown good preliminary results in ECD patients carrying this mutation [12, 13].

Radiological findings of thoracic involvement of ECD have been described in previous reports; however, to our knowledge, a comprehensive study examining a large series of patients has not been reported [14–17]. The goal of our study was to prospectively characterize the thoracic CT imaging findings in 61 ECD patients as well as to investigate the association of these findings with the $BRAF^{V600E}$ mutation in the 58 patients whose paraffin-embedded tissue samples were interpretable for $BRAF^{V600E}$ sequencing.

Materials and methods

Patient selection

This was a prospective study approved by the institutional review board at the National Human Genome Research Institute (NHGRI), Bethesda, MD, USA (clinicaltrials.gov identifier: NCT01417520) and was Health Insurance Portability and Accountability Act (HIPAA) compliant. Written informed consent was obtained from all patients prior to their participation in the study.

ECD patients of any gender and ethnicity, aged 2–80 years, with biopsy-confirmed ECD based on pathology of affected organs were eligible to enrol in this study. Patients with suspected diagnosis of ECD that was not confirmed by biopsy, those who had another form of histiocytosis, children under the age of 2 years old, and pregnant women were excluded from the study. Sixty-one patients (mean age: 52 years; range: 19–74 years) who fulfilled these criteria were included in the present study. This group was comprised of 46 male (mean age: 54 years; range: 34–74 years) and 15 female patients (mean age: 49 years; range: 19–64 years). Clinical findings related to 60 patients included in our study population were previously reviewed by Estrada-Veras et al. [7].

Patient imaging

Eligible patients were consecutively imaged at the National Institutes of Health between 2011 and 2016 under protocol 11-HG-0207, 'Clinical and Basic Investigations into Erdheim-Chester disease'. Multidetector computed tomography (MDCT) scans of the chest were performed in all patients (Siemens Definition n=5, Siemens Somatom Definition AS n=3, Toshiba Aquilion ONE n=49, GE Medical Systems LightSpeed Ultra n=3, GE Medical Systems Discovery ST n=1) with reconstructed section thicknesses of both 2 mm and 5 mm (gantry rotation time, 0.8 s; and beam pitch, 0.5). Five patients underwent contrast-enhanced CT (Iopidamol 300mg/ml (Isovue-300) Bracco Diagnostics, Monroe Township, NJ, USA) and 56 patients underwent non-contrast CT.

Image analysis

Two fellowship-trained radiologists, with 8 and 3 years of experience, reviewed 61 chest CT images independently. The reviewing radiologists were aware of the pathology-proven diagnosis but were blinded to all clinical, imaging and genetic ($BRAF^{V600E}$ status) information. Each patient had only one chest CT to be reviewed, thus a time interval between reads was not necessary to eliminate recall bias as no patient had multiple studies. Disagreements were resolved by discussion and subsequent agreement between the two readers. Chest CT images were evaluated for histiocytic infiltration involving the lung parenchyma and airways (interstitial lung disease, lung nodules, ground glass opacities, honeycombing and bronchial wall thickening), pleura (thickening, effusions) and mediastinum (mediastinal infiltration,

lymphadenopathy, involvement of the heart chambers, pericardial effusion/thickening and vascular sheathing) [14].

Genetic studies

Archived paraffin-embedded tissue samples were available from 60 ECD patients for analysis of $BRAF^{V600E}$ mutations. Polymerase chain reaction-based sequencing of exons 11, 12 and 15 (n=25), allele-specific polymerase chain reaction (n=14), pyrosequencing on a QIAGEN PyroMark Q24 system (Valencia, CA, USA) (n=20), or whole exome sequencing (n=1), was used to identify the $BRAF^{V600E}$ mutations in the 60 samples.

Statistical analysis

Statistical analysis was performed using R Statistical Software (Foundation for Statistical Computing, v3.4.0, Vienna, Austria). Data were normally distributed based on the Shapiro-Wilk test. Continuous variables are expressed as mean ± standard deviation (SD). Categorical variables are expressed as frequency with percentage. Percentage differences in thoracic pathology between subjects with and without $BRAF^{V600E}$ mutations were compared with the Chi-square or Fisher's exact test and odds ratios (ORs) with 95% confidence intervals (CI), as appropriate. A two-sided p-value < 0.05 was considered to indicate a significant difference.

Results

Demographics

Median age at the time of initial visit was 52 years for males and 50 years for females. Sixteen patients had respiratory manifestations (dyspnea in 11 cases, chronic cough in three and recurrent sinusitis in two); however, the majority (45 patients) were asymptomatic. Data concerning smoking and environmental exposure history were collected from the cohort during the initial history and physical examination. Smoking status was classified as either former, current smoker (pack-years) or never smoker. Patient demographic data is summarized in Table 1.

Imaging findings

Of the 61 ECD patients imaged in our study, 55 patients (90%) had lung parenchymal and/or airways involvement, nine (15%) had pleural involvement and 38 (62%) had mediastinal involvement on MDCT. The radiological findings are summarized in a color map table (Fig. 1). The color map table is a visual tool that describes the radiological and genomic findings of each patient together.

Table 1 Demographic characteristics and environmental data in the Erdheim-Chester disease (ECD) patient cohort

Characteristic		No. of Patients	Percentage
Sex			
Female		15	25% (15/61)
Male		46	75% (46/61)
Smoking and environmental history	Never smoker	53	87% (53/61)
	Former smoker	4	7% (4/61)
	Current smoker	4 (7-20 P/Y)	7% (4/61)
	Asbestos exposure	5	8% (5/61)

Lung parenchyma and airways involvement

The most common parenchymal finding among our ECD patients was interlobular septal thickening, which was present in 42 patients (69%). Interlobular septal thickening was divided into diffuse and focal interlobular septal thickening. Diffuse interlobular septal thickening was defined as involvement of both lungs, seen in 16 patients (26%), and tended to be peripheral and lower lung predominant. Twenty-six cases (43%) had focal involvement that involved only one lung or a portion of one lung (Fig. 2).
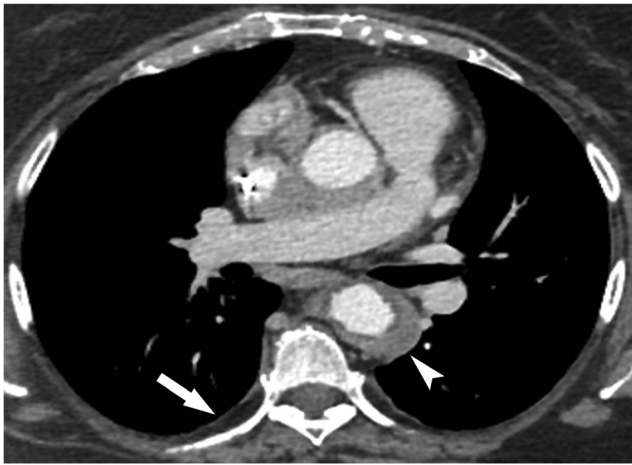
Thirty-eight patients (62%) with pulmonary involvement exhibited nodules in the lungs (Fig. 3). The nodules were solid, well-circumscribed lesions, measuring 5 mm or less in size (mean size of 3 mm) and were classified by the pattern of distribution: nodules located in subpleural regions (n=22, 36%), nodules in lung parenchyma (n=8, 13%) and nodules present in both regions (n=8, 13%). Nodules in the lung parenchyma were centrilobular in distribution. Subpleural nodules were associated with the fissures and in the periphery of the lungs. Both subpleural nodules and centrilobular nodules in the lung parenchyma had an upper lobe predominance (82% of subpleural nodules and 63% of parenchymal nodules).

Ground glass opacities were observed in 22 patients (36%), manifesting in a subpleural and/or peribronchovascular pattern in the majority of cases. One patient demonstrated remarkably diffuse patchy peribronchovascular ground glass opacities accompanied by perivascular cysts (lymphoid interstitial pneumonia); however, with concurrent Sjögrens syndrome, these findings could not be attributed to ECD.

No patient presented with honeycombing on MDCT imaging. Eight patients (13%) had long-segment, circumferential bronchial wall thickening. The bronchial wall thickening was scattered, did not involve all lobes, and had no particular lobar predominance.

Fig. 1 Color map showing the *BRAF* mutation and pulmonary and mediastinal involvement in a population of 61 Erdheim-Chester disease (ECD) patients. (The dashed cells indicate absence of tissue sample. Dark purple cells in the "Interlobular Septal Thickening" row indicate diffuse involvement and light purple cells indicate focal involvement)

Pleural involvement

Nine patients (15%) had pleural involvement. Four patients (7%) had pleural effusions and one (2%) had pleural thickening (Fig. 4). The remaining four patients (7%) demonstrated both pleural effusion and pleural thickening on MDCT imaging.

Mediastinal involvement

The mediastinum was assessed for the presence of lymphadenopathy, infiltration, myocardial wall thickening and vascular

Fig. 2 Interlobular septal thickening in Erdheim-Chester disease (ECD) patients. **a** Axial CT image of the chest without contrast in lung windows in a 68-year-old male shows focal interlobular septal thickening (arrows) and bilateral pleural effusions. **b** Axial CT image of the chest without contrast in lung windows in a 65-year-old female patient shows diffuse interlobular thickening (arrows), left greater than right

Fig. 3 **a** Axial non-contrast CT image in lung windows in a 62-year-old male Erdheim-Chester disease (ECD) patient shows lung nodules along the fissure (arrow). **b** Axial non-contrast CT image in lung windows in a 62-year-old male ECD patient shows subpleural nodules (arrows)

Fig. 4 Axial contrast-enhanced chest CT image in a 65-year-old female Erdheim-Chester disease (ECD) patient shows bilateral pleural thickening (arrow) and aortic sheathing (arrowhead)

and esophageal sheathing. A total of 38 patients (62%) demonstrated mediastinal involvement. Seven patients (11%) presented with both mediastinal lymphadenopathy and mediastinal infiltration. Thickening of the wall of the right atrium was observed in nine patients (15%). Four patients (6%) demonstrated mild cardiomegaly, three of whom also had right atrial wall thickening on contrast-enhanced CT. With respect to the prevalence of vascular sheathing (Fig. 5), the right coronary artery was most frequently involved (n=21, 34%), followed by sheathing of the thoracic aorta in 18 patients (30%). None of the patients with vascular sheathing demonstrated luminal narrowing. Table 2 demonstrates the distribution of thoracic aortic involvement.

Other vascular sheathing was present within the cohort; two patients (3%) demonstrated sheathing of the superior vena cava and one patient (2%) had sheathing of the right pulmonary artery. None of the patients included in the present cohort showed vascular aneurysm. Thoracic CT showed the presence of pericardial effusion in six patients (10%), pericardial thickening in five patients (8%) and both in two patients (3%). Esophageal sheathing was not found in our patient population.

Genetic findings

The association between radiological presentations and the genetic findings was evaluated in 31 out of 58 patients (53%) who had interpretable samples for *BRAF* sequencing. Although a statistically significant association was found between the frequency of some thoracic findings and $BRAF^{V600E}$, not all of them were pathophysiologically relevant. The only finding that showed a significant positive association with $BRAF^{V600E}$ was sheathing of the RCA ($p = 0.01$; OR = 4.69).

Table 3 summarizes the results of statistical analysis for association of $BRAF^{V600E}$ mutation and thoracic involvement.
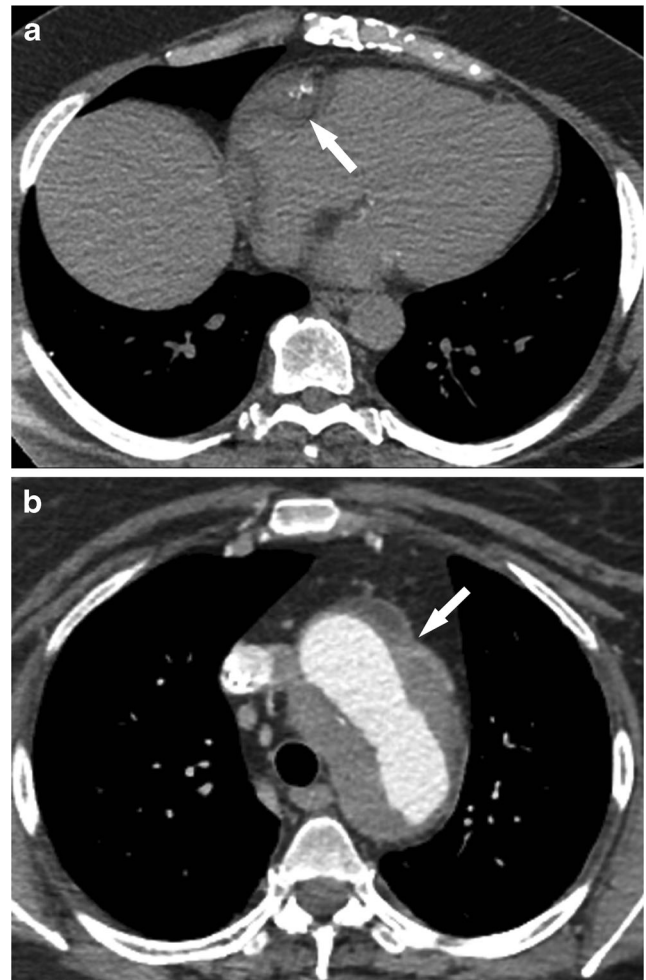
Fig. 5 **a** Non-contrast axial chest CT image in soft tissue windows in a 48-year-old male Erdheim-Chester disease (ECD) patient demonstrates sheathing of the right coronary artery (arrow). Atherosclerotic calcification is noted within the right coronary artery. **b** Contrast-enhanced axial chest CT image in a 46-year-old male ECD patient shows involvement of the aortic arch (arrow) by ECD

Discussion

ECD is a multisystemic disease that presents with various manifestations. This large, single-centre study of thoracic involvement in 61 ECD patients describes the various extraskeletal thoracic manifestations of ECD. In addition, we

Table 2 Distribution of thoracic aortic involvement in Erdheim-Chester disease (ECD) patients

Thoracic aortic involvement	No. of patients	Percentage
Descending aorta	15	25% (15/61)
Aortic arch	12	20% (12/61)
Ascending aorta	8	13% (8/61)
Entire thoracic aorta	6	10% (6/61)

Table 3 Statistical analysis showing the association of thoracic imaging finding of Erdheim-Chester disease (ECD) and $BRAF^{V600E}$ status

Imaging findings			$BRAF^{V600E}$ + n = 31	$BRAF^{V600E}$ − n = 27	p-value	Odds ratio (95% CI)
Non-Vascular	Lung	Interlobular septal thickening	24 (77.4)	17 (63.0)	0.36	2.02 (0.64–6.36)
		Bronchial wall thickening	3 (9.7)	5 (18.5)	0.45	0.47 (0.10–2.19)
		Ground glass opacities	9 (29.0)	12 (44.4)	0.35	0.51 (0.17–1.51)
		Subpleural nodules	15 (48.4)	13 (48.1)	0.99	1.01 (0.36– 2.84)
		Non-subpleural nodules	5 (16.1)	11 (40.7)	0.04	0.28 (0.08–0.95)
		Pleural effusions	4 (12.9)	4 (14.8)	0.99	0.85 (0.19–3.79)
		Pleural thickening	2 (6.5)	3 (11.1)	0.66	0.55 (0.09–3.58)
	Mediastinum	Mediastinal adenopathy	3 (9.7)	4 (14.8)	0.69	0.62 (0.12–3.04)
		Mediastinal infiltration	3 (9.7)	3 (11.1)	0.99	0.86 (0.16–4.65)
	Cardiac	Cardiomegaly	3 (9.7)	1 (3.7)	0.62	2.79 (0.27–28.50)
		Right atrium wall thickening	7 (22.6)	2 (7.4)	0.15	3.65 (0.69–19.33)
		Pericardial effusions	5 (16.1)	3 (11.1)	0.71	1.54 (0.33–7.14)
		Pericardial thickening	5 (16.1)	2 (7.4)	0.43	2.40 (0.43–13.55)
Vascular		Sheathing of thoracic aortic artery	13 (41.9)	5 (18.5)	0.09	3.18 (0.95–10.60)
		Sheathing of coronary arteries	16 (51.6)	5 (18.5)	0.01	4.69 (1.41–15.58)
		Sheathing of pulmonary arteries	1 (3.2)	0 (0.0)	0.99	NA
		Sheathing of superior vena cava	1 (3.2)	1 (3.7)	0.99	0.87 (0.05–14.56)

evaluated the association between these thoracic manifestations of ECD and the presence of the $BRAF^{V600E}$ mutation.

Our study showed that 90% of the patients in our cohort had pulmonary findings. Previous smaller studies have shown a range of pulmonary involvement in ECD patients ranging from 50% to 89% [8, 14–16, 18]. The higher frequency of pulmonary findings detected in our study might reflect improved imaging quality allowing detection of more subtle findings. In addition, our prospective protocol called for scans of asymptomatic patients, allowing the detection of pulmonary abnormalities in individuals with minimal or no symptoms. Compared to the prior study by Estrada-Veras et al. on the same cohort population, the higher rate of pulmonary involvement in the present study (52% vs. 90%) relates to the evaluation for other pulmonary findings in addition to pulmonary fibrosis, including pulmonary nodules, bronchial wall thickening and ground glass opacities.

Among the patients of our cohort, interlobular septal thickening (69%) and small nodules (62%) were the most frequent pulmonary findings. Interestingly, we found that a common distribution of pulmonary nodules in ECD patients was a subpleural pattern (Fig. 4), not previously reported. This pattern may correspond to the lymphangitic distribution of histiocytic infiltration that has been described on histopathology, but it remains uncertain if these represent small nodules of histiocytes or small intraparenchymal lymph nodes infiltrated with histiocytes [19]. Detection of these micronodular opacities depends on both the quality of imaging and high accuracy of reading and interpretation and may have been overlooked on older CT scans with thicker slices.

Pleural involvement, secondary to thickening of the visceral pleura by histiocyte infiltration and/or fibrosis [19], was seen in 15% (nine patients) of our study group, as opposed to 41% reported by Arnaud et al. [16] and 40% by Brun et al. [14]. The lower proportion of pleural involvement reported in our study may be explained by the fact that all the study population had been diagnosed prior to admission to our institution, and the majority of them had received some form of treatment before this evaluation.

Cardiovascular lesions in ECD involve periadventitial histiocytic infiltration of cardiac chambers and blood vessels, which appears as soft tissue density surrounding the involved structure on CT. This is one of the characteristic features of ECD and can lead to vascular stenosis and ischemia. Cardiovascular involvement has been reported as the second most common manifestation in ECD after skeletal involvement and can be associated with a poorer prognosis [2, 3, 14, 20–22]. Our study showed that infiltration of histiocytes around the right coronary artery (34%) was the most frequent vascular finding followed by thoracic aorta involvement (30%). None of the patients in our cohort with vascular sheathing had vascular stenosis on chest CT and have not demonstrated symptoms of ischaemic complications at this point in time.

A high prevalence of the $BRAF^{V600E}$ mutation, an activating proto-oncogene, in ECD patients has been described by recent studies as a potential target for effective treatment [9, 13]. However, the association between $BRAF^{V600E}$ and ECD complications has not been reported. We found that the $BRAF^{V600E}$ mutation had a strong positive association with

the frequency of RCA sheathing in this study. In a similar paper reporting the abdominal manifestations of this ECD cohort, a significant association was found between periaortic infiltration of the abdominal aorta and BRAF status. However, the same association was not found with regards to the thoracic portion of the aorta. This suggests that patients with the gene mutation are at risk of periaortic infiltration of the abdominal aorta, more so than the thoracic aorta [23]. Careful attention should be paid to this mutation in planning regular imaging surveillance for RCA stenosis; therapeutic interventions, based upon *BRAF* testing, could improve the prognosis of ECD.

Limitations

The present study has a number of limitations. While it was prospective in nature, the CT images were acquired using different acquisition protocols due to various admission dates, thereby creating some possible discrepancies in comparability or interpretation. Although many patients presented with radiological evidence of pulmonary involvement and all had a tissue biopsy confirming the ECD, the tissue biopsies in our patient cohort came from various tissues (depending on where the most disease was present) and only two of the tissue biopsies were lung tissue. In terms of cardiovascular involvement, because our study was limited to evaluation of chest CTs, we did not have functional cardiac information to assess cardiovascular complications such as wall motion abnormalities, decreased left ventricular ejection fraction and ischemia.

Conclusion

In conclusion, this large single-centre study of 61 patients with ECD describes both the thoracic imaging manifestations as well as their association with the $BRAF^{V600E}$ mutation. The high prevalence of pulmonary and cardiovascular involvement in ECD found in this study indicates that evaluation with thoracic CT plays a crucial role in detecting and monitoring ECD progression and should be a part of the routine comprehensive assessment of ECD patients. Our study also shows a positive association between RCA sheathing and the $BRAF^{V600E}$. Future studies evaluating the clinical implications of this association are warranted.

Compliance with ethical standards

References

1. Haroche J, Arnaud L, Amoura Z (2012) Erdheim–Chester disease. Curr Opin Rheumatol 24(1):53–59
2. Abdelfattah AM, Arnaout K, Tabbara IA (2014) Erdheim-Chester disease: a comprehensive review. Anticancer Res 34(7):3257–3261
3. Haroche J, Arnaud L, Cohen-Aubart F et al (2013) Erdheim-Chester disease. Rheum Dis Clin N Am 39(2):299–311
4. Campochiaro C, Tomelleri A, Cavalli G, Berti A, Dagna L (2015) Erdheim-Chester disease. Eur J int Med 26(4):223–229
5. Swerdlow SH, Campo E, Pileri SA et al (2016) The 2016 revision of the World Health Organization classification of lymphoid neoplasms. Blood 127(20):2375–2390
6. Mazor RD, Manevich-Mazor M, Shoenfeld Y (2013) Erdheim-Chester Disease: a comprehensive review of the literature. Orphanet J Rare Dis 8(1):137
7. Estrada-Veras JI, O'Brien KJ, Boyd LC et al (2017) The clinical spectrum of Erdheim-Chester disease: an observational cohort study. Blood Adv 1(6):357–366. https://doi.org/10.1182/bloodadvances.2016001784
8. Diamond EL, Dagna L, Hyman DM et al (2014) Consensus guidelines for the diagnosis and clinical management of Erdheim-Chester disease. Blood 124(4):483–492
9. Haroche J, Charlotte F, Arnaud L et al (2012) High prevalence of BRAF V600E mutations in Erdheim-Chester disease but not in other non-Langerhans cell histiocytoses. Blood 120(13):2700–2703. https://doi.org/10.1182/blood-2012-05-430140
10. Janku F, Vibat CRT, Kosco K et al (2014) BRAF V600E mutations in urine and plasma cell-free DNA from patients with Erdheim-Chester disease. Oncotarget 5(11):3607

11. Cohen Aubart F, Emile JF, Maksud P, et al (2016) Efficacy of the MEK inhibitor cobimetinib for wild-type BRAF Erdheim-Chester disease. B J Haematol

12. Hyman DM, Puzanov I, Subbiah V et al (2015) Vemurafenib in multiple nonmelanoma cancers with BRAF V600 mutations. N Engl J Med 373(8):726–736

13. Haroche J, Cohen-Aubart F, Emile J-F et al (2014) Reproducible and sustained efficacy of targeted therapy with vemurafenib in patients with BRAF(V600E)-mutated Erdheim-Chester disease. J Clin Oncol 33(5):411–418

14. Brun A-L, Touitou-Gottenberg D, Haroche J et al (2010) Erdheim-Chester disease: CT findings of thoracic involvement. Eur Radiol 20(11):2579–2587

15. Antunes C, Graça B, Donato P (2014) Thoracic, abdominal and musculoskeletal involvement in Erdheim-Chester disease: CT, MR and PET imaging findings. Insights Into imaging 5(4):473–482

16. Arnaud L, Pierre I, Beigelman-Aubry C et al (2010) Pulmonary involvement in Erdheim-Chester disease: A single-center study of thirty-four patients and a review of the literature. Arthritis Rheum 62(11):3504–3512

17. Dion E, Graef C, Haroche J et al (2004) Imaging of thoracoabdominal involvement in Erdheim-Chester disease. AJR Am J Roentgenol 183(5):1253–1260

18. Wittenberg KH, Swensen SJ, Myers JL (2000) Pulmonary involvement with Erdheim-Chester disease: radiographic and CT findings. AJR Am J Roentgenol 174(5):1327–1331

19. Rush WL, Andriko JAW, Galateau-Salle F et al (2000) Pulmonary pathology of Erdheim-Chester disease. Mod Pathol 13(7):747–754

20. Gianfreda D, Palumbo AA, Rossi E et al (2016) Cardiac involvement in Erdheim-Chester disease: an MRI study. Blood 128(20):2468–2471

21. Haroche J, Amoura Z, Dion E et al (2004) Cardiovascular involvement, an overlooked feature of Erdheim-Chester disease: report of 6 new cases and a literature review. Medicine 83(6):371–392

22. Serratrice J, Granel B, De Roux C et al (2000) "Coated aorta": a new sign of Erdheim-Chester disease. J Rheumatol 27(6):1550–1553

23. Nikpanah M, Kim L, Mirmomen SM et al (2018) Abdominal involvement in Erdheim-Chester disease (ECD): MRI and CT imaging findings and their association with BRAF^{V600E} mutation. Eur Radiol :1–9. https://doi.org/10.1007/s00330-018-5326-1